Clinical and Experimental Ophthalmology 2003; **31**: 147–154

Original Article

Confocal imaging of the human keratocyte network using the vital dye 5-chloromethylfluorescein diacetate

C Anthony Poole PhD,[1] Nigel H Brookes MSc(Hons)[2] and Gillian M Clover FRANZCO[1]
Departments of [1]Anatomy with Radiology and [2]Ophthalmology, Faculty of Medical and Health Sciences, University of Auckland, Auckland, New Zealand

ABSTRACT

Background: The human corneal stroma consists of intercalated layers of collagen and keratocytes. These cells are known to maintain the stroma and aid in repair but it is likely they have other crucial roles throughout the cornea. The complexity of their anatomy is revealed in this study by *ex vivo in situ* images of the human keratocyte covering a range of ages.

Methods: Human donor corneas of different ages were stained with 5-chloromethylfluorescein diacetate (CMFDA), a dye that is anchored and retained within the cell cytoplasm. The tissue was fixed, sectioned, mounted, and then imaged using a confocal laser scanning microscope at various magnifications and tissue planes. The digital image sets were transferred to multifunction image processing software for analysis and production of 3-D stereo images of keratocyte networks throughout the stroma.

Results: High quality images of CMFDA-stained cells revealed differences in the structure and orientation of keratocytes in the anterior, central and posterior stroma, which did not differ throughout the age-range studied. This method reveals very fine cell process ramifications not previously visualized, orientated in lateral and anteroposterior directions, and it confirms the potential for multidirectional communication between keratocyte networks.

Conclusions: This qualitative study found consistency of keratocyte morphology in the normal human cornea throughout life. It confirmed differences in keratocyte anatomy, and the potential for rapid cellular communication by multiple interconnecting processes supporting cohesive keratocyte activity. This high-resolution 3-D microscopic study should assist in identifying gross deviant cellular behaviour in post-surgical and disease states.

Key words: cell processes, confocal microscopy, 5-chloromethylfluorescein diacetate, human cornea, keratocytes, 3-D reconstruction.

INTRODUCTION

The keratocyte is not a quiescent cell. Rather, it has a dynamic role not only in the development of the corneal stroma but also in its maintenance and its reaction to wounding and disease states.[1] In the last decade, studies utilizing new techniques and novel approaches have furthered understanding of the disposition of the keratocyte throughout the stroma, and its relationship to the collagen fibrils and the glycoproteins in different parts of the cornea.[1–6]

Earlier anatomical studies provided the concept of intercalated layers of collagen and keratocytes, but did not give substantial anatomical evidence that the keratocytes connect with each other via cell processes, other than in a lateral orientation.[7] This model precluded the possibility that the cell layers could interact directly with each other by intercellular channels, or that keratocyte populations could act cohesively in all dimensions, except perhaps through secreted messenger substances diffusing via the extracellular matrix. Subsequently, anatomical and immunohistochemical studies provided evidence that keratocytes link in both lateral and anteroposterior directions[2,3,8–10] via intercellular communication channels, and could potentially act cohesively throughout the cornea, or at least within variable 3-D functional groups. Such an integrated system of cells communicating via gap junctions[8–10] provides an anatomical substrate for coordinated maintenance of the corneal stroma, for cohesive reaction to injury or disease, and for programmed cell death and replacement.

The evidence for keratocyte activity has grown:[1,11–13] the presence of organelles such as mitochondria, the golgi apparatus and rough endoplasmic reticulum, indicate that these cells can actively manufacture and secrete substances used for the production, maintenance and repair of proteoglycans,

■ *Correspondence:* Mr Nigel H Brookes, Department of Ophthalmology, Faculty of Medical and Health Sciences, University of Auckland, Private Bag 92019, Auckland, New Zealand. Email: n.brookes@auckland.ac.nz

stromal collagen and keratocytes. There is a differential in the presence of these organelles between the anterior and posterior cornea, perhaps indicating activities specialized to the position of the keratocyte within the cornea.[11,12] Three cellular layers with distinct morphological characteristics in the anterior, central and posterior stroma have been identified in the porcine cornea which may relate to the disposition and type of collagen surrounding the keratocytes, to specific functions, and to transparency requirements in these regions.[2,3] Membrane fenestrations at the cell margins have been related to collagen fibrils and it has been suggested that collagen fibrils might be adherent to keratocytes at fenestrated sites.[1] These are the putative sites where collagen is being manufactured and laid down, thereby influencing the disposition of the collagen fibrils in relation to individual keratocytes and their cell processes within each cellular plane.

It is not surprising that interest in the keratocyte has increased in recent years; corneal refractive surgery, initially radial keratotomy then photorefractive keratectomy (PRK) and laser *in situ* keratomileusis (LASIK), has complications of postoperative corneal haze and sometimes unpredictable shifts in the refractive correction achieved. Such outcomes require further investigation of corneal wound healing in relation to refractive procedures and of the interaction of the anterior keratocyte with the overlying epithelium and underlying stroma. The finding of keratocyte apoptosis in relation to corneal epithelial removal in PRK was revealing, and indicated that there is probably a controlling or interactive relationship between the corneal epithelium and the anterior keratocyte. These observations have been supported by the finding of growth factors produced by the keratocyte and by the epithelium that influence the behaviour of these closely related cellular populations.[14–21]

As refractive surgery gains further acceptance there is an ongoing need to reduce complications and suboptimal refractive outcomes. It is desirable to detect early, and manage beneficially, potential aberrant reactions to PRK by modifying unsatisfactory reactions of the cornea to the procedure. To achieve this, it is essential that our knowledge of the normal microanatomy, disposition and functions of the human keratocyte be well established.

There have been numerous *in vivo* confocal microscopy studies of the human cornea, but the resolution is limited to cell bodies and major processes.[17,22,23] However, the true complexity of keratocyte anatomy was revealed to the authors when studying the porcine cornea stained with vital dyes. When examined by *ex vivo in situ* confocal microscopy, each keratocyte formed extensive fine ramifications of its cell processes throughout the three dimensional complexity of the corneal stromal matrix.[2,3]

In the current study we present *ex vivo in situ* images of the human keratocyte stained with vital dyes, and assess a range of ages for variations that might occur throughout the lifespan of the human cornea. It is anticipated that such information might assist surgeons to interpret keratocyte images obtained by *in vivo* confocal microscopy, to detect abnormal keratocyte behaviour in disease states and postoperatively, and to determine the efficacy of remedial therapies.

Table 1. Details of the human corneas used

Specimen	Age (years)	Cause of death	Death-to-staining time (hours)
1	10	Accident: fall on rocks	24
2	35	Suicide: CO poisoning	19
3	45	Suicide: CO poisoning	23
4	50	Ischaemic heart disease	4
5	65	Ischaemic heart disease	20
6	67	Heart (no specific details)	22
7	69	Pulmonary embolism	20

METHODS

Tissue collection and CMFDA labelling

Experiments were performed using corneas removed from human donors, collected but deemed unsuitable for transplantation by the New Zealand National Eye Bank (Table 1). These were transferred to the laboratory, where a central trephine (6 mm in diameter) was taken from the centre of each cornea. This trephine was cut into three pieces and placed, epithelial side down, into separate wells of a 24-well multiplate containing cornea transportation medium (CTM) at 34°C, to ensure corneal maintenance under optimal conditions. This media consists of standard cornea organ culture medium supplemented with 5% dextran (500 000 MW) to minimize swelling of the corneas.[24]

After 15 min equilibration, the media was aspirated and replaced with media containing 25 μmol/L 5-chloromethylfluorescein diacetate (CMFDA, CellTracker-Green; Molecular Probes, Eugene, OR, USA).[5] The corneas were left to stain overnight in the dark at 4°C without agitation. Following CMFDA loading, the stain solution was carefully aspirated, and the tissue gently washed three times with fresh media. The corneal samples were fixed in freshly prepared 2% paraformaldehyde for 10 min, and washed again with media. For long-term storage, each sample was equilibrated in an Epindorf tube containing media supplemented with 20% dimethyl sulphoxide (DMSO) and frozen at –20°C. For short-term storage up to 3 days, fixed corneas were immediately embedded in OCT compound (Tissue Tek; Sakura Finetek, Torrance, CA, USA), and prepared for cryosectioning.

Cryosectioning

Prior to cryomicrotomy each corneal hemisphere was thawed and washed in media to remove residual DMSO. The tissue was frozen in OCT, in either an anteroposterior or lamellar orientation, and 30 μm cryosections collected serially through the whole thickness of the cornea. Frozen sections were dried onto numbered slides, and representative

sections were selected using conventional fluorescence microscopy. Selected sections were mounted in VectaSheild (Vector Laboratories, Burlingame, CA, USA) for imaging.

Confocal microscopy, image acquisition and processing

Keratocytes were imaged using a Leica TCS 4d confocal laser scanning microscope (Leica, Heidelberg, Germany) fitted with a krypton-argon laser source and recommended filter sets. To facilitate comparison with previous light microscopic studies using Calcein-AM,[2,3] all sections were initially scanned at lower magnification, and a *z*-series data set of 10–30 images collected through 10–30 μm of the *z*-axis. To better define the interaction between extremely fine keratocyte processes, a number of selected fields within each section were imaged at high magnification. A *z*-series of 10–20 optical sections was collected and the scanning parameters for each image presented are included with each figure caption.

Digitized image data sets were processed in VoxelView (Vital Images, Plymouth, MN, USA) on a Silicon Graphics IRIS Indigo R4000 workstation with XS-24 graphics (Silicon Graphics, Mountain View, CA, USA) to construct a 3-D representation of the data set, using 'projection lighting' to create a surface rendered, 3-D effect. The reconstructed images were rotated ±4 degrees about the *x*-axis to produce pairs of stereo images of the keratocyte networks in different regions of the stroma.

RESULTS

In all the corneas sampled, irrespective of their age and their contra-indicators for the donor program, CMFDA labelling consistently showed brightly fluorescent keratocytes contrasted against the extracellular matrix, which showed negligible background staining, or autofluorescence. Although anteroposterior sections were prepared for each cornea, lamellar sections were significantly easier to process and provided a high degree of cellular detail.

Keratocyte organization in the anteroposterior plane

The anteroposterior distribution of keratocytes is summarized in Fig. 1. A low-resolution full-thickness composite (Fig. 1a) shows brightly stained epithelial and endothelial layers, with strongly contrasted keratocytes forming ramping connections throughout the entire depth of the stroma. Details from the anterior stroma beneath the epithelium (Fig. 1b) revealed a significantly higher keratocyte density than a comparable magnification of the central stroma (Fig. 1c). Anterior keratocytes formed an extensive network of branching and interconnecting cell bodies and cell processes that dominated the matrix, but showed a relatively poor lamellar organization. By comparison, central stromal keratocytes showed variable orientation and inclination of the flattened cell bodies within the lamellar framework. They also showed a high degree of mutual interconnectivity between cell processes, which extended large distances between adjacent keratocytes in alternating lamallae. Details from the posterior stroma adjacent to Descemet's membrane and the endothelium (Fig. 1d) also revealed distinct keratocyte morphologies, and a higher cell density than the bulk of the central stroma. Keratocyte cell bodies appeared larger and were interconnected by short cell processes projecting laterally and obliquely to contact neighbouring cell bodies or processes.

These morphological distinctions between anterior, central and posterior keratocytes were subsequently used for more specific analysis of lamellar sections taken serially from the anterior to the posterior surfaces of the cornea. Sections immediately adjacent to Bowman's membrane and Descemet's membrane were considered representative of anterior and posterior keratocyte populations, respectively. Sections from the middle of the series were considered representative of central stromal keratocytes.

Keratocyte organization in the lamellar plane

A comparison of anterior, central and posterior keratocytes in the lamellar plan from donors aged 10, 45 and 69 years, is shown in Fig. 2. Although some variation was to be expected between different donors, the pattern of anterior, central and posterior keratocyte density and morphology was consistent across the age groups included in this study. Anterior keratocytes formed a dense network of cell bodies and cell processes extensively interconnected with neighbouring keratocytes (Figs 2a,d,g). Unstained areas of the stromal matrix were reduced in the anterior region of the cornea, which contrasted markedly with the central stroma where unstained matrix dominated the field (Figs 2b,e,h). The cell bodies of central keratocytes were flattened and clearly delineated in a variety of oblique orientations. Long slender cell processes extended from the cell bodies and coursed through the unstained lamellar matrix to contact keratocytes in different cellular planes. The density of posterior keratocytes was always greater than that of the central keratocytes (Figs 2c,f,i), the cells having large cell bodies and extensive short processes connecting neighbouring keratocytes.

The interlamellar interconnectivity of anterior, central and posterior keratocytes was best illustrated in stereo-pair reconstructions (Fig. 3). In the anterior region of the stroma, there was a high degree of overlap between cell bodies at different depths of the anterior stroma (Fig. 3a). Lateral and oblique projections of the short cytoplasmic cell processes created a network of contacts throughout the anterior stroma. None of the preparations examined showed evidence of keratocytes extending cell processes across Bowman's membrane to make direct contact with the basal cells of the epithelium.

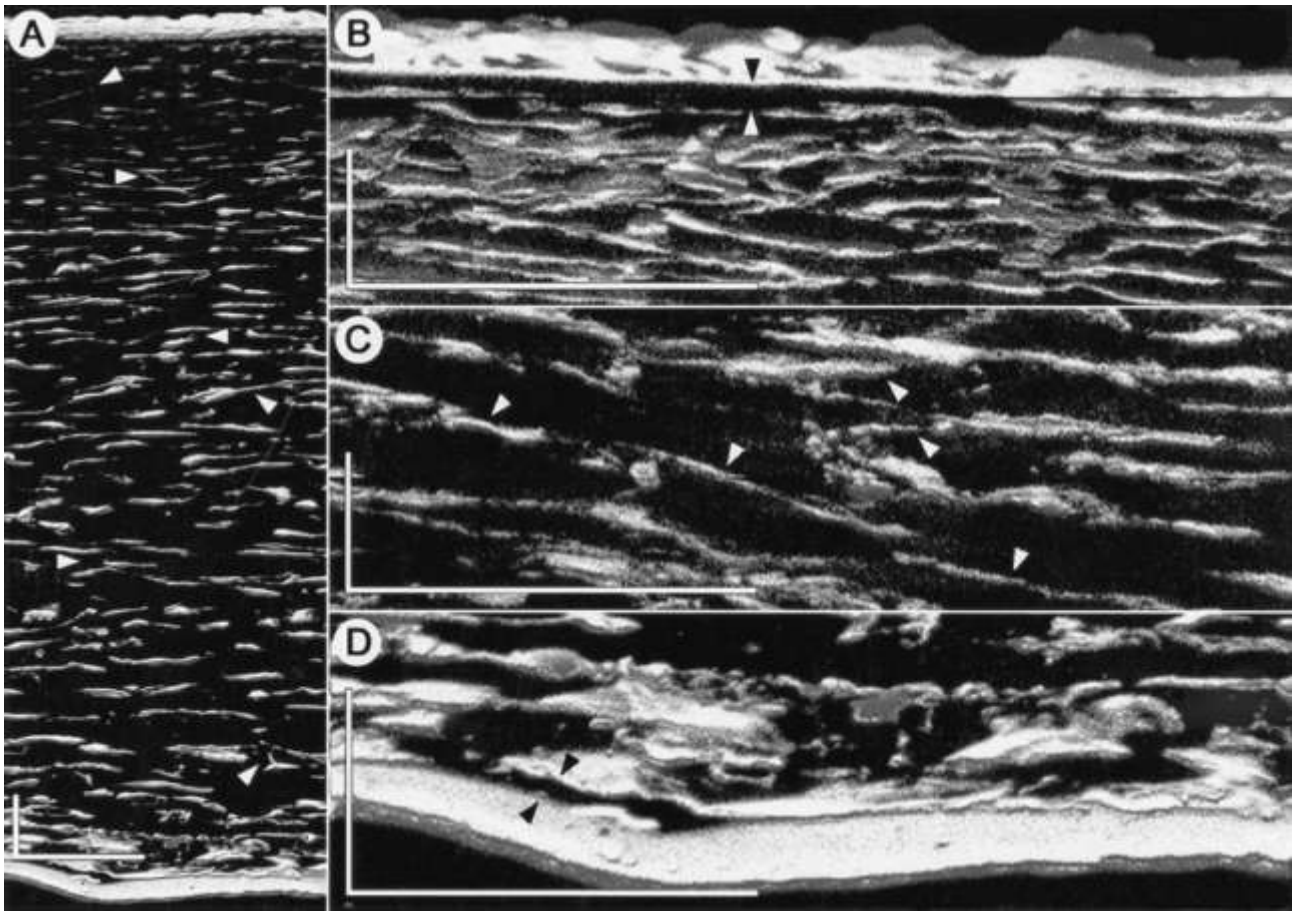

Figure 1. Anteroposterior views of human keratocytes stained with 5-chloromethylfluorescein diacetate. (a) Field view through the full thickness of the corneas (Man, 65 years; composite of 7 volumes, each 18 optical sections through 35.80 μm; 18/35.80 μm). Only cell bodies were evident at low magnification, although ramping interconnections between adjacent cell bodies were common (▲). (b) Detail of the epithelium, Bowman's membrane (▲), the high cell density and poor lamellar organization in the anterior stroma (Woman, 67 years; 15/29.40 μm). (c) Detail of the central stroma (Woman, 35 years; 18/18.30 μm), where the low cell density highlights ramping interconnections extending both laterally and anteroposteriorly (▲). (d) Detail of the endothelium, Descemet's membrane (▲) and the posterior stroma where cell density is high and extensively interconnected. All scale bars represent 100 μm.

In the central stroma (Fig. 3b), where keratocyte density was much reduced, cell bodies are flattened and variably orientated, and interconnected laterally and obliquely by attenuated cell processes that form a variety of cell process to cell process and cell process to cell body contacts.

Posteriorly (Fig. 3c), we confirmed the narrow range over which posterior keratocytes could be identified (3–4 cells thick), with care being taken to examine sections in which portions of the endothelium and Descemet's membrane could be accurately identified at the margins. Keratocyte cell bodies appeared more rounded in contour, and were interconnected by short cell processes that projected laterally and obliquely to contact neighbouring cell bodies or processes in all planes. None of the preparations examined showed evidence of keratocytes extending cell processes across Descemet's membrane to make direct contact with the basal surface of the endothelial monolayer.

These differences between the three keratocyte subpopulations identified were clearly illustrated in comparable high-resolution reconstructions of cells from each region (Fig. 4). Large, variably shaped and orientated cell bodies and numerous short cell processes characterized anterior keratocytes. Together they formed a variety of cell process to cell process, cell process to cell body and cell body to cell body contacts, which dominated the anterior stroma (Fig. 4a). In the central stroma, where cell density was clearly lower, cell bodies also showed variable shape and orientation, and maintained some cell body to cell body contacts (Fig. 4b). However, continuity with adjacent keratocytes was largely maintained through an attenuated network of cell process to cell process contacts (Fig. 4b). The cell bodies of posterior keratocytes appeared 'swollen' when compared to anterior and central keratocytes (Fig. 4c). They were fringed by a number of short cell processes and flat extensions of CMFDA-stained cytoplasm, which formed thin fenestrated areas adjacent to parts of the cell body (Fig. 4c).

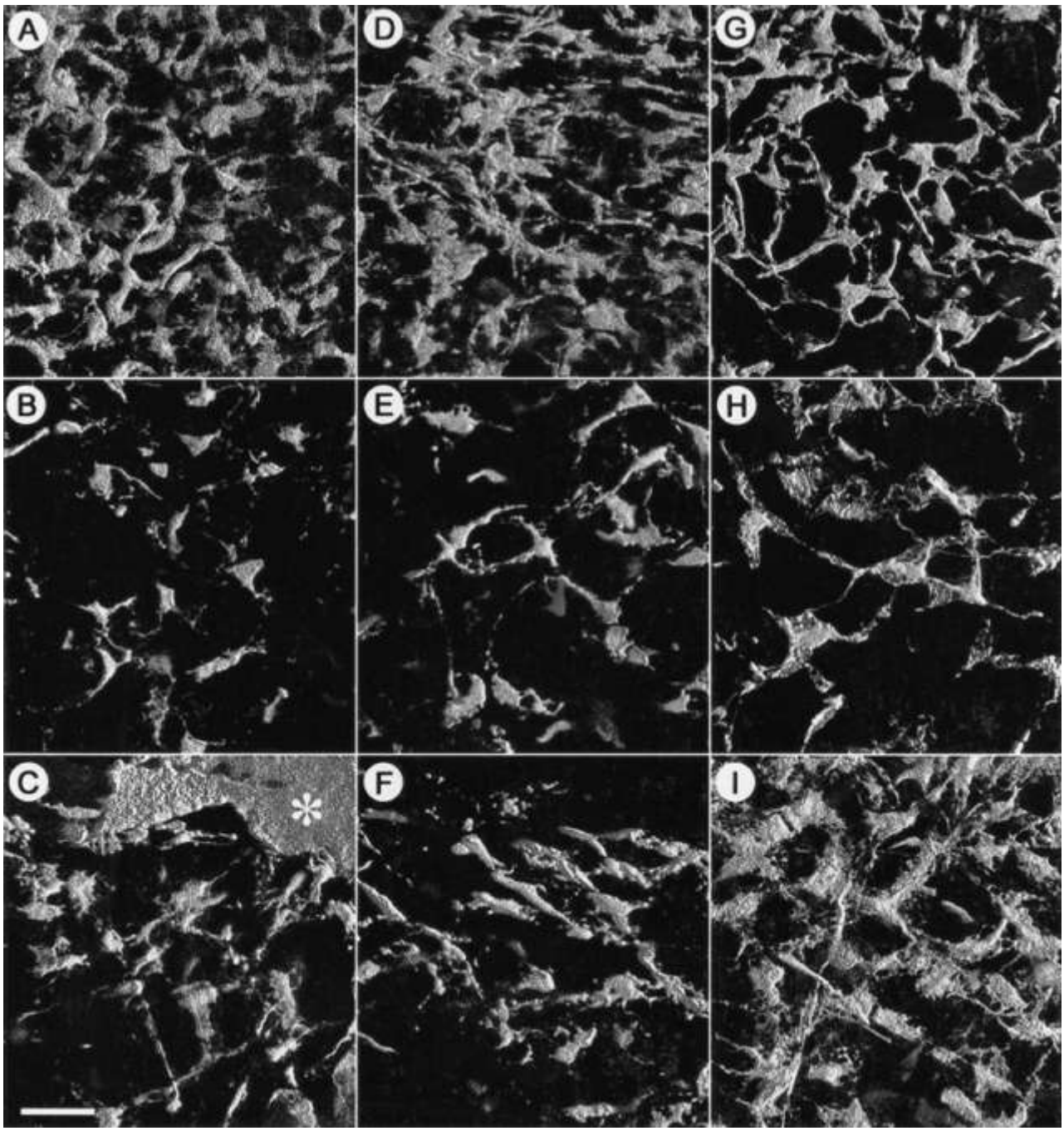

Figure 2. Low power lamellar views of (a,d,g) anterior, (b,e,h) central and (c,f,i) posterior keratocytes from individuals aged (a–c) 10 years, (d–f) 45 years and (g–i) 69 years. Volumes ranging from 17/17.05 μm to 20/22.97 μm are presented. Similar patterns of cell density and morphology were evident at all ages, although individual variations were common. Keratocyte density and interconnectivity was maximal in (a,d,g) the anterior stroma, high in (c,f,i) the posterior stroma and least in (b,e,h) the central stroma. In (c), part of Descemet's membrane is shown (*) to indicate its close proximity to posterior keratocytes, but was removed from the rendered volumes of (f) and (i). Scale bar = 50 μm.

Discussion

The advantages of CMFDA in combination with confocal laser scanning microscopy have been previously discussed.[3,5] In summary, the images obtained are of very high quality due to dye anchoring and retention throughout the cell cytoplasm enabling the finest cell process ramifications and complex cell borders such as fenestrations to be readily visualized at high magnifications. In addition, the samples can be fixed, which allows accurate cutting of sections up to 50 μm thick within desired cellular planes. This technique compares favourably with the use of Calcein-AM in unfixed tissue, which is subject

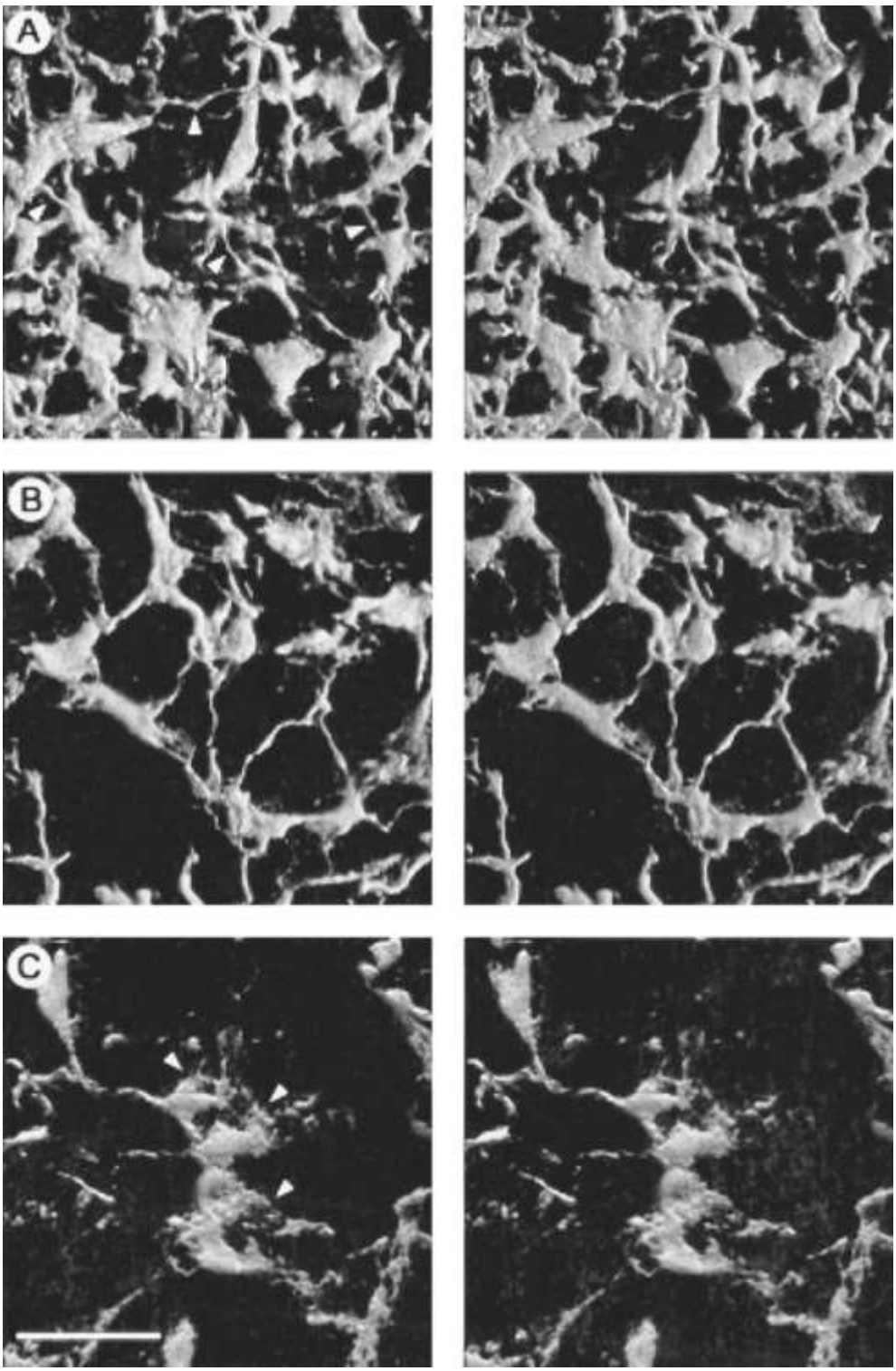

Figure 3. Lamellar-view stereopairs of (a) anterior, (b) central and (c) posterior keratocytes at intermediate magnifications. In the anterior stroma (Man, 50 years; 22/21.95 μm), cell bodies overlap and are interconnected by short cell processes (▲). Keratocyte density was reduced in the central stroma (Woman, 35 years; 25/25.30 μm), with cell bodies interconnected obliquely by long cell processes. In the posterior stroma (Man, 60 years; 20/20.15 μm), keratocyte cell bodies appeared more rounded, with thin fenestrae (▲) and fine cell processes projecting laterally and obliquely. Scale bar = 50 μm.

to distortion, degradative artefacts and background tissue fluorescence during the course of tissue examination.[2,24,25]

These observations of the human keratocyte expand on our previous porcine study using CMFDA, and are in advance of other studies using Calcein-AM. Confocal microscopy of CMFDA-stained samples enables serial thin optical sectioning and image reconstruction in three dimensions, which further enhances our ability to visualize undisturbed keratocyte morphology *in situ*. Knowledge of the morphology of the three keratocyte subpopulations identified in high resolution in the porcine model, and confirmed by this study as being present also in the human, is critical if we are to understand the physiology of this vital component of the visual system.

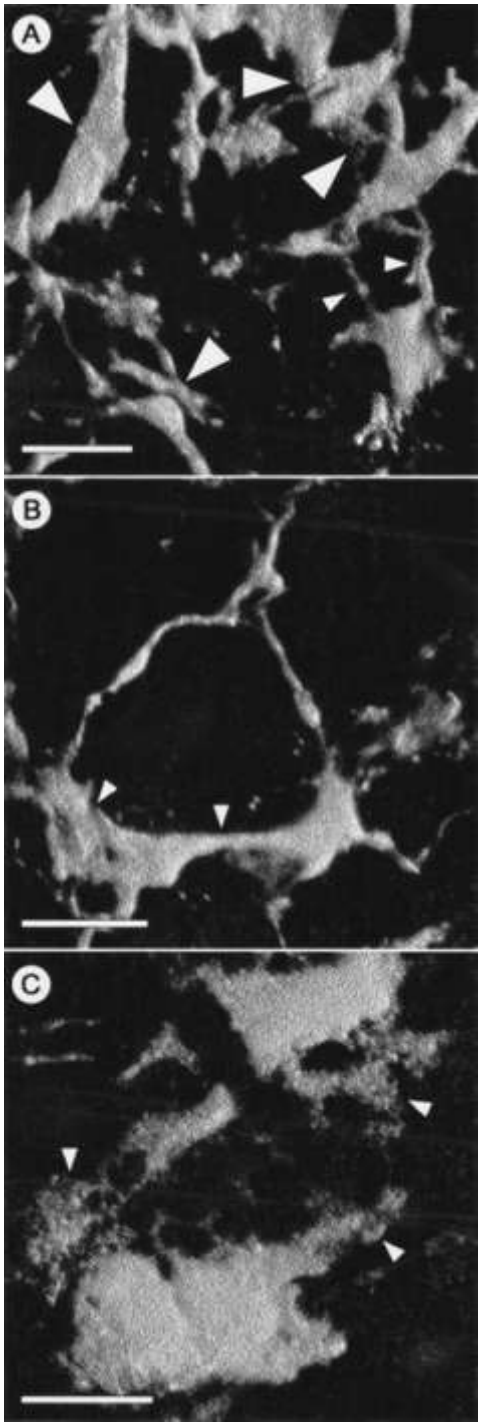

Figure 4. (right) High-magnification lamellar views of the three keratocyte subpopulations identified in this study. (a) Anterior stroma showing cell body to cell body (large arrows), cell process to cell body (medium arrows) and cell process to cell process (small arrows) contacts (Man, 50 years; 22/21.95 μm). (b) Central stroma showing cell body contacts (arrows), the unique staining profile each cell process, and their pseudo-random orientation within the matrix (Woman, 35 years; 25/25.30 μm). (c) Posterior stroma showing cell body contacts, short cell processes and fenestrated sheets of CMFDA-stained cytoplasm, which extend from most keratocytes in this region (arrows) (Man, 50 years; 19/18.73 μm). Scale bars = 20 μm.

The death-to-staining times for the human corneas used in this study were not ideal for retention of optimal cell viability and integrity of morphology. Nevertheless, the images obtained compare favourably with the detail obtained in fresh young porcine corneas.

Our understanding of the underlying cell biology of tissue reactions to LASIK and PRK in the human cornea is limited.[26,27] Postoperative *in vivo* confocal microscopy studies have characterized some gross changes in keratocyte and stromal morphology and corneal innervation.[17,18,28,29] The present study aimed to provide information regarding the consistency of keratocyte morphology in the normal cornea throughout life by comparing the morphology within a wide range of donor cornea ages. Although the changes observed following refractive surgery have been generally characterized, the similarity of the existing cell populations in different age groups prior to surgical intervention, and their reactions to surgical damage, have not been recorded. Currently, refractive surgery is undertaken principally in the 3rd and 4th decades of life, but this may change over time. Four of our selected corneas fall within the age range 10–50 years, but do not differ substantially from those corneas aged 65–69 years, particularly in relation to the cell subpopulations present and types of cell-to-cell contacts they form. Volumetric analyses have not been undertaken to-date as such analyses would be of little value unless many human corneas were available for study. Using high-resolution techniques, we aimed to provide detailed qualitative information about the consistency and intricacy of the human keratocyte morphology in a range of ages.

In particular, we demonstrated the variable orientation and size of the human anterior keratocyte population, which is dense and has a larger number of cells compared with central and posterior layers. Viewed in the lamellar plane, the shape of anterior keratocytes appears particularly variable, which could relate principally to cell orientation rather than variation in the individual cell body volume. Thus observations that keratocytes in this layer become larger following PRK or LASIK could be due to: (i) cellular re-orientation to a different plane; (ii) damaged cells 'rounding up' with loss of cell processes and increased cell body size during the process of apoptosis; or (iii) a different cell type being present which is larger, such as the myofibroblast.[15,19,21]

Finally, images of keratocyte organization in the anteroposterior plane throughout all cell layers demonstrate morphologically the potential for interconnectivity between keratocytes throughout the human stroma. Comparative animal studies have confirmed the presence of gap junctions and associated proteins revealed by immunohistochemical, functional and electron microscopy studies.[1,3,8–10] Hence the behaviour of the anterior keratocyte should not be perceived in isolation from the rest of the stroma, nor from the overlying epithelium, as there are both intercellular and extracellular routes whereby the behaviour of cells could be influenced by cytokines produced in response to direct injury to one part of the stroma.

In summary, in this high-resolution study, we defined the characteristic shape, size and orientation of the human keratocyte cell bodies throughout the stroma, and the morphology of cell process and cell body contacts that form a 3-D syncytium throughout the corneal stroma. The knowledge of the human keratocyte microanatomy over a range of ages provided by this study should assist in identifying gross deviant cellular behaviour in post-surgical and disease states by *in vivo* or *ex vivo in situ* confocal microscopy.

ACKNOWLEDGEMENTS

This research was funded in part by The Maurice and Phyllis Paykel Trust and The New Zealand National Eye Bank (NHB/GMC), and The Sir William and Lady Stevenson Trust (GMC). C Anthony Poole is a Senior Research Fellow of the Health Research Council of New Zealand.

REFERENCES

1. Muller LJ, Pels L, Vrensen GFJM. Novel aspects of the ultrastructural organisation of human corneal keratocytes. *Invest Ophthalmol Vis Sci* 1996; **13**: 2557–67.
2. Poole CA, Brookes NH, Clover GM. Keratocyte networks visualised in the living cornea using vital dyes. *J Cell Sci* 1993; **106**: 685–92.
3. Poole CA, Brookes NH, Clover GM. Confocal imaging of the keratocyte network in porcine cornea using the fixable vital dye 5-chloromethylfluorescein diacetate. *Curr Eye Res* 1996; **15**: 165–74.
4. Nishida T, Yasumoto K, Otori T, Desaki J. The network structure of corneal fibroblasts in the rat as revealed by scanning electron microscopy. *Invest Ophthalmol Vis Sci* 1988; **29**: 1887–90.
5. Poole CA, Brookes NH, Gilbert RT *et al.* Detection of viable and non-viable cells in connective tissue explants using the fixable fluoroprobes 5-chloromethylfluorescein diacetate and ethidium homodimer-1. *Conn Tiss Res* 1995; **33**: 233–41.
6. Petroll WM, Jester JV, Cavanagh HD. *In vivo* confocal imaging: general principles and applications. *Scanning* 1994; **16**: 131–49.
7. Hogan MJ, Alvarado JA, Weddell JE. *Histology of the Human Eye*. London: WB Saunders, 1971.
8. Clover GM, Brookes NH, Poole CA. Simultaneous co-localisation of keratocytes and connexins 43 and 50. *Invest Ophthalmol Vis Sci* 1998; **39/4**: S453.
9. Jester JV, Barry PA, Lind GJ, Petroll WM, Garana R, Cavanagh HD. Corneal keratocytes: *in situ* and *in vitro* organisation of cytoskeletal contractile proteins. *Invest Ophthalmol Vis Sci* 1994; **35**: 730–43.
10. Watsky MA. Keratocyte gap junctional communication in normal and wounded rabbit corneas and human corneas. *Invest Ophthalmol Vis Sci* 1995; **36**: 2568–76.
11. Stockwell RA. Morphometry of cytoplasmic components of mammalian articular chondrocytes and corneal keratocytes. Species and zonal variations of mitochondria in relation to nutrition. *J Anat* 1991; **175**: 251–61.
12. Moller-Pedersen T, Ehlers NA. Three-dimensional study of the human corneal keratocyte density. *Curr Eye Res* 1995; **14**: 459–64.
13. Petroll WM, Boettcher K, Barry P, Cavanagh HD, Jester JV. Quantitative assessment of anteroposterior keratocyte density in the normal rabbit cornea. *Cornea* 1995; **14**: 3–9.
14. Vesaluoma N, Perez-Santonja J, Petroll WM, Linna T, Alio J, Tervo T. Corneal stromal changes induced by myopic LASIK. *Invest Ophthalmol Vis Sci* 2000; **41**: 369–76.
15. Szerenyi KD, Wang X, Gabrielian K, McDonnell PJ. Keratocyte loss and repopulation of anterior corneal stroma after de-epithelialization. *Arch Ophthalmol* 1994; **112**: 973–6.
16. Moller-Pedersen T, Cavanagh HD, Petroll WM, Jester JV. Neutralizing antibody to TGF-β modulates stromal fibrosis but not regression of photoablative effect following PRK. *Curr Eye Res* 1998; **17**: 736–47.
17. Moller-Pedersen T, Vogel M, Li HF, Petroll WM, Cavanagh HD, Jester JV. Quantification of stromal thinning, epithelial thickness, and corneal haze after photorefractive keratectomy using *in vivo* confocal microscopy. *Ophthalmology* 1997; **104**: 360–68.
18. Linna TU, Vesaluoma MH, Perez-Santonja JJ, Petroll WM, Alio JL, Tervo TMT. Effect of myopic LASIK on corneal sensitivity and morphology of subbasal nerves. *Invest Ophthalmol Vis Sci* 2000; **41**: 393–7.
19. Helena MC, Baerveldt F, Kim W-J, Wilson SE. Keratocyte apoptosis after corneal surgery. *Invest Ophthalmol Vis Sci* 1998; **39**: 276–83.
20. Wilson SE, He Y-G, Weng J, Li Q, Vital M, Chwang EL. Epithelial- and endothelial-derived interleukin-1 (IL-1) modulates corneal tissue organisation and wound healing response through induction of keratocyte apoptosis. *Invest Ophthalmol Vis Sci* 1995; **36**: S866.
21. Masur SK, Erenburg I, Dinh TT, Connors R Jr, Dewal HS. TGF-β secretion induces myofibroblast differentiation in cultured corneal fibroblasts. *Invest Ophthalmol Vis Sci* 1995; **36**: S867.
22. Essepian JP, Rajpal RK, Azar DT *et al.* The use of confocal microscopy in evaluating corneal wound healing after excimer laser keratectomy. *Scanning* 1994; **16**: 300–4.
23. Patel SV, McLaren JW, Camp JJ, Nelson LR, Bourne WM. Automated quantification of keratocyte density by using confocal microscopy *in vivo*. *Invest Ophthalmol Vis Sci* 1999; **40**: 320–26.
24. Armitage WJ, Moss SJ. Storage of corneas for transplantation. In: Easty DL, ed. *Current Ophthalmic Surgery*. London: Baillère Tindal, 1990; 193–9.
25. Hahnel C, Somodi S, Weiss DG, Guthoff RF. The keratocyte network of human cornea: a three-dimensional study using confocal laser scanning fluorescence microscopy. *Cornea* 2000; **19**: 185–93.
26. Kaufman SC, Maitchouk DY, Chiou AGY, Beuerman RW. Interface inflammation after laser *in situ* keratomileusis: Sands of the Sahara syndrome. *J Cataract Refract Surg* 1998; **24**: 1589–93.
27. Moller-Pedersen T, Cavanagh HD, Petroll WM, Jester JV. Corneal haze development after PRK is regulated by volume of stromal tissue removal. *Cornea* 1998; **17**: 627–39.
28. Mitooka K, Ramirez M, Maguire LJ *et al.* Keratocyte density of central human cornea after laser *in situ* keratomileusis. *Am J Ophthalmol* 2002; **133**: 307–14.
29. Erie JC, Patel SV, McLaren JW, Maguire LJ, Ramirez M, Bourne WM. Keratocyte density *in vivo* after photorefractive keratectomy in humans. *Trans Am Ophthalmol Soc* 1999; **97**: 221–40.